UNIVERSITÀ DEGLI STUDI DI TORINO

Latest results from the KASCADE-Grande experiment

A. Chiavassa[c], W.D. Apel[a], J.C. Arteaga-Velázquez[b], K. Bekk[a], M. Bertaina[c], J. Blümer[a,d], H. Bozdog[a], I.M. Brancus[e], E. Cantoni[c,f,1], F. Cossavella[d,2], C. Curcio[c], K. Daumiller[a], V. de Souza[g], F. Di Pierro[c], P. Doll[a], R. Engel[a], J. Engler[a], B. Fuchs[d], D. Fuhrmann[h,3], H.J. Gils[a], R. Glasstetter[h], C. Grupen[i], A. Haungs[a], D. Heck[a], J.R. Hörandel[j], D. Huber[d], T. Huege[a], K.-H. Kampert[h], D. Kang[d], H.O. Klages[a], K. Link[d], P. Łuczak[k], M. Ludwig[d], H.J. Mathes[a], H.J. Mayer[a], M. Melissas[d], J. Milke[a], B. Mitrica[e], C. Morello[f], J. Oehlschläger[a], S. Ostapchenko[a,4], N. Palmieri[d], M. Petcu[e], T. Pierog[a], H. Rebel[a], M. Roth[a], H. Schieler[a], S. Schoo[a], F.G. Schröder[a], O. Sima[l], G. Toma[e], G.C. Trinchero[f], H. Ulrich[a], A. Weindl[a], J. Wochele[a], J. Zabierowski[k]

[a] *Institut für Kernphysik, KIT - Karlsruher Institut für Technologie, Germany*
[b] *Universidad Michoacana, Instituto de Física y Matemáticas, Morelia, Mexico*
[c] *Dipartimento di Fisica, Università degli Studi di Torino, Italy*
[d] *Institut für Experimentelle Kernphysik, KIT - Karlsruher Institut für Technologie, Germany*
[e] *National Institute of Physics and Nuclear Engineering, Bucharest, Romania*
[f] *Osservatorio Astrofisico di Torino, INAF Torino, Italy*
[g] *Universidade São Paulo, Instituto de Física de São Carlos, Brasil*
[h] *Fachbereich Physik, Universität Wuppertal, Germany*
[i] *Department of Physics, Siegen University, Germany*
[j] *Dept. of Astrophysics, Radboud University Nijmegen, The Netherlands*
[k] *National Centre for Nuclear Research, Department of Cosmic Ray Physics, Lodz, Poland*
[l] *Department of Physics, University of Bucharest, Bucharest, Romania*

Abstract

The KASCADE-Grande experiment operated at KIT from January 2004 to November 2012, measuring EAS generated by primary cosmic rays in the $10^{16} - 10^{18} eV$ energy range. The experiment detected, for each single event, with a high resolution, the total number of charged particles (N_{ch}) and of muons (N_{μ}).

In this contribution we present the latest results about:

(i) the measurement of the all particle energy spectrum, discussing the influence of the hadronic interaction model used to derive the energy calibration of the experimental data.

(ii) The energy spectra derived separating the events according to the N_{μ}/N_{ch} ratio. This technique allowed us to unveil a steepening of the spectrum of heavy primaries at $E \sim 10^{16.92\pm0.04} eV$ and a hardening of the spectrum of light primaries at $E \sim 10^{17.08\pm0.08} eV$.

(iii) The elemental spectra (for five mass groups) obtained applying a detailed unfolding analysis technique.

(iv) A search for large scale anisotropies.

Keywords: Cosmic Rays, Extensive Air Showers, Knee, Spectra

1. Introduction

Measurements of the cosmic-rays all-particle and individual elemental spectra, of the primary chemical composition and of the anisotropies in the primaries arrival directions are the tools to understand the phenomenology of cosmic rays. The KASCADE-Grande experiment was built to investigate the energy range from 10^{16} to $10^{18} eV$ with the main goal of searching for a change of slope in the primary spectrum of the heavy particles and to investigate the possible transition from a galactic to an extra-galactic origin of cosmic rays in this energy range.

The results obtained at lower energies by KASCADE[1] and EAS-TOP[2] as well as by other experiments suggest that the knee in the primary energy spectrum observed at $3-4\times10^{15} eV$ is due to a break in the spectrum of light elements (Z$\leq$ 6). Several models foresee a rigidity dependence of such breaks. Therefore, a knee of the heavy component is expected around $10^{17} eV$. Such features can only be investigated by precise measurements both of the all-particle spectrum (i.e. the spectrum of the entire event sample) and of the spectra of different mass groups (i.e. the spectra of event samples obtained applying a primary mass dependent selection).

The evolution with energy of the primary chemical composition brings also relevant informations concerning the transition from a galactic origin of the primary radiation to an extragalactic one. Most of the astrophysical models identify in a change toward a composition dominated by light (mainly protons) primaries a sign of such a transition. It is therefore of main importance to perform composition studies in a wide energy range and with high resolution.

Email address: `andrea.chiavassa@to.infn.it` (A. Chiavassa)
[1] now at: Istituto Nazionale di Ricerca Metrologia, INRIM, Torino.
[2] now at: DLR Oberpfaffenhofen, Germany.
[3] now at: University of Duisburg-Essen, Duisburg, Germany.
[4] now at: University of Trondheim, Norway.

Preprint submitted to NIM A RICAP-2013 *August 1, 2013*

In addition a search for large scale anisotropies in the arrival directions of cosmic rays is performed, that is an observable very sensible to the propagation of the primaries in the galactic magnetic fields. The foreseen effect is very low (of the order of $10^{-3} - 10^{-2}$) and is hidden by counting differences induced by pressure and temperature variations. To take into account such effects we have performed the search following the East-West method[3].

In this contribution we will present the updated results obtained for the all-particle[4], light[5] and heavy[6] primary energy spectra; we will discuss the elemental spectra obtained unfolding the $N_{ch} - N_{\mu}$ spectrum[7]; and we will show the upper limits derived from a search for large scale anisotropies[8].

2. Experimental setup

The multi-detector experiment KASCADE[9] (located at 49.1° n, 8.4° e, 110m a.s.l.) was extended to KASCADE-Grande in 2003 by installing a large array of 37 stations consisting of $10m^2$ scintillation detectors each, the layout is shown in figure 1. KASCADE-Grande[10] provides an area of $0.5km^2$ and operates jointly with the existing KASCADE detectors. The joint measurements with the KASCADE muon tracking devices are ensured by an additional cluster (Piccolo) located close to the center of KASCADE-Grande and deployed for fast trigger purposes. For results of the muon tracking devices see [11].

The Grande detectors are sensitive to charged particles, while the KASCADE array detectors measure the electromagnetic component and the muonic component separately. These muon detectors enable to reconstruct the total number of muons on an event-by-event basis also for Grande triggered events.

Basic shower observables like the core position, angle-of-incidence, and total number of charged particles (N_{ch}) are provided by the measurements of the Grande stations. The Grande array accuracy in the EAS parameters reconstruction is measured comparing, on an event by event basis, the values independently determined by the KASCADE and by the Grande arrays. A resolution of $5m$ on the core position, of 0.7° on the arrival direction, and of 15% on the total number of charged particles (with a systematic difference lower than 5%) has been achieved. The total number of muons is determined using the core position reconstructed by the Grande array and the muon densities measured by the KASCADE muon array detectors. The resolution on the N_{μ} EAS parameter is evaluated reconstructing simulated events, a ∼ 20% accuracy has been achieved. More details on the experimental setup and on the event reconstruction can be found in[10].

Full efficiency for triggering and reconstruction of air-showers is reached at a primary energy of $10^{16}eV$, slightly varying on the cuts needed for the reconstruction of the different observables[10].

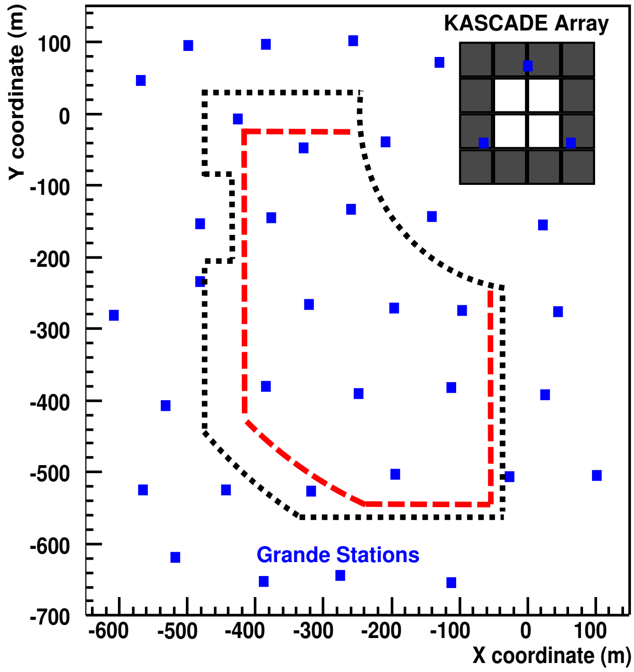

Figure 1: Layout of the KASCADE-Grande experiment. The KASCADE array and the distribution of the 37 stations of the Grande array are shown. The 192 muon detectors are placed in the outer 12 clusters of the KASCADE array (hatched area). The dashed line shows the fiducial area selected for the all-particle and heavy mass group spectra analysis. The dotted line indicates the area used for the measurement of the light mass group spectrum.

3. Results

3.1. All particle energy spectrum

The energy of the primary particle that originated the detected EAS is determined by the KASCADE-Grande experiment by means of the N_{ch} and N_{μ} observables[4], combining these two variables indeed we can lower the dependence from the chemical composition of the primary particles. This is obtained evaluating for each event the so called k parameter, that is essentially a measurement of the ratio between the muon and the charged particles numbers.

$$k = \frac{\log_{10}(N_{ch}/N_{\mu}) - \log_{10}(N_{ch}/N_{\mu})_H}{\log_{10}(N_{ch}/N_{\mu})_{Fe} - \log_{10}(N_{ch}/N_{\mu})_H} \quad (1)$$

$$\log_{10}(N_{ch}/N_{\mu})_{H,Fe} = c_{H,Fe} \log_{10} N_{ch} + d_{H,Fe} \quad (2)$$

From its definition is clear that k is a number centered around zero (one) for proton (iron) generated events, if expressed as a function of N_{ch} for Monte Carlo events, assuming intermediate values for all other primaries. The values of the k parameters are tuned by a full EAS and detector simulation, the analysis reported in [4] is based on the QGSJetII-02[12] hadronic interaction model. Having calculated, for each event, the k parameter the primary energy is estimated from the N_{ch} value:

$$\log_{10}(E/GeV) = [a_H + (a_{Fe} - a_H) \cdot k] \log_{10}(N_{ch}) + b_H + (b_{Fe} - b_H) \cdot k \quad (3)$$

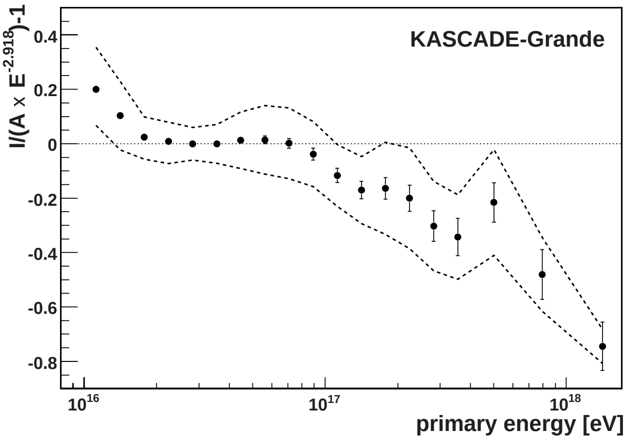

Figure 2: The all-particle energy spectrum obtained with KASCADE-Grande. The residual intensity after multiplying the spectrum with a factor of $E^{2.918}$ is displayed as well as the band of systematic uncertainty.

To take into account the shower evolution in atmosphere the parameters, $a_{H,Fe}, b_{H,Fe}, c_{H,Fe}, d_{H,Fe}$, contained in the k and E expressions are derived in five different angular intervals, whose upper limits are: $16.7°, 24.0°, 29.9°, 35.1°$ and $40.0°$. The values of the parameters can be found in[4].

The all-particle energy spectrum is then measured in the five different angular bins. As shown in[4] these spectra are slightly shifted, indicating that the EAS evolution in atmosphere is not correctly described by the simulations. Nevertheless these differences are inside the experimental uncertainties and thus we mediate them to obtain the all particle energy spectrum measured in zenith angle range from 0° to 40°. The residuals of the all-particle energy spectrum multiplied by a factor, in such a way that the middle part of the spectrum becomes flat are shown in figure 2.

The measured spectrum cannot be described by a single power law: a hardening around $10^{16} eV$ and a steepening at $\log_{10}(E/eV) = 16.92 \pm 0.10$ are observed. The statistical significance of the steepening is 2.1σ, here the change of the spectral slope is from $\gamma = -2.95 \pm 0.05$ to $\gamma = -3.24 \pm 0.08$. The same spectral features are meanwhile confirmed by the Tunka-133[13] and Ice-Top[14] experiments.

This procedure relies on the EAS simulation and thus depends on the high-energy hadronic interaction model used. To evaluate the systematic effects introduced in the all-particle spectrum measurement[15] the same procedure has been repeated using events simulated with the SIBYLL2.1[16], EPOS1.99[17] and QGSJetII-04[18] hadronic interaction models.

Applying the energy calibration functions, obtained by each model, to the measured data the all-particle energy spectra for the five zenith angle bins are obtained for the four previously mentioned models; for all of them, except QGSJetII-04, an unfolding procedure has been applied. Different sources of uncertainty affect the all-particle energy spectrum. A detailed description is reported in[4]. They take into account: a) the angular dependence of the parameters appearing in the energy calibration functions of the different angular ranges. b) The possible bias introduced in the energy spectrum by different primary compositions. c) The spectral slope of Monte Carlo used in the simulations. d) The reconstruction quality of N_{ch} and N_{μ}. The total systematic uncertainty is $\sim 20\%$ at the threshold ($E = 10^{16} eV$) and $\sim 30\%$ at the highest energies ($E = 10^{18} eV$) almost independently from the interaction model used to interpret the data. The final all-particle spectrum of KASCADE-Grande is obtained (see figure 3) by combining the spectra for the individual angular ranges. Only those events are taken into account, for which the reconstructed energy is above the energy threshold for the angular bin of interest. In general the shape of the energy spectrum is very similar for all models, however, a shift in flux is clearly observed which amounts to $\sim 25\%$ increase in case of SIBYLL2.1 and $\sim 10\%$ decrease in case of EPOS1.99. This is the consequence of the energy shift assigned on an event-by-event basis. This result gives an estimation of the systematic uncertainty on the experimental flux due to the hadronic interaction model used to interpret the data, and it is essentially independent of the technique used to derive the flux, namely averaging the fluxes obtained in different angular bins. The shift in the assigned energy to the data is also visible in the hardening around $\sim 2 \times 10^{16} eV$ and in the steepening around $10^{17} eV$ which look shifted among the models in general agreement with the energy shift. This result indicates that the features seen in the spectrum are not an artifact of the hadronic interaction model used to interpret the data but they are in the measured data. In the overlapping region, KASCADE-Grande data are compatible inside the systematic uncertainties with KASCADE data interpreted with the same model.

3.2. Energy spectra of individual mass groups

The k parameter previously defined can also be used to separate the events in samples generated by two different primary mass groups. To emphasize the features of the heavy elements we selected the electron-poor events with $k_{ep}(E) \geq (k_C(E) + k_{Si}(E))/2$, i.e. events with a k value greater that the mean value of the expectations for C and Si primaries (QGSJetII-02[12] based simulation). The spectra of these event samples are shown in figure 4, the band indicates changes of the spectra when the cut is varied by one standard deviation in the $k_{ep}(E)$ definition.

The reconstructed spectrum of the electron-poor events shows a distinct knee like feature at about $8 \times 10^{16} eV$. Applying a fit of two power laws to the spectrum interconnected by a smooth knee[19] results in a statistical significance of 3.5σ that the entire spectrum cannot be described with a single power-law. The change of the spectral index is $\Delta\gamma = -0.48 \pm 0.05$ from $\gamma = -2.76 \pm 0.02$ to $\gamma = -3.24 \pm 0.05$ with the break position at $\log_{10}(E/eV) = 16.92 \pm 0.04$. The spectrum of the electron-rich events (corresponding, with this cut definition, to light and medium mass primaries) is compatible with a single power law with slope index $\gamma = -3.18 \pm 0.01$. A recovery to a harder spectrum at energies greater than $10^{17} eV$ cannot be excluded by this analysis.

To increase the statistics and deeply investigate this possible hardening of the light primaries spectrum a larger fiducial

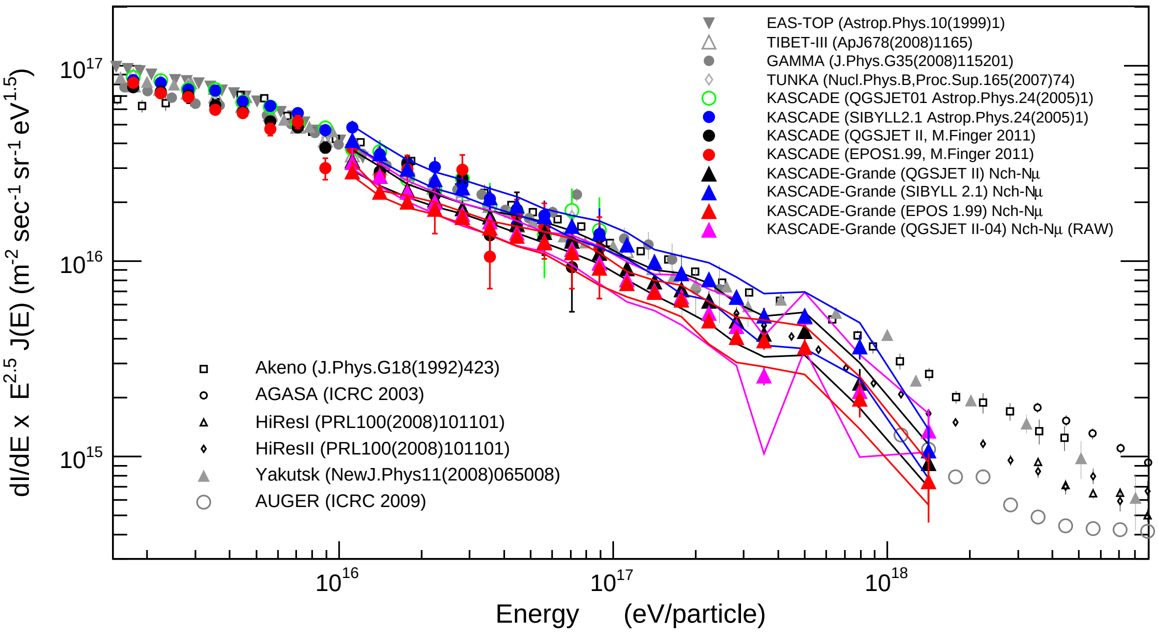

Figure 3: Comparison of the all-particle energy spectrum obtained with KASCADE-Grande data based on SIBYLL2.1 (blue), QGSJetII-02 (black), QGSJetII-04 (pink) and EPOS1.99 (red) models to results of other experiments. The band denotes the systematic uncertainties in the flux estimation

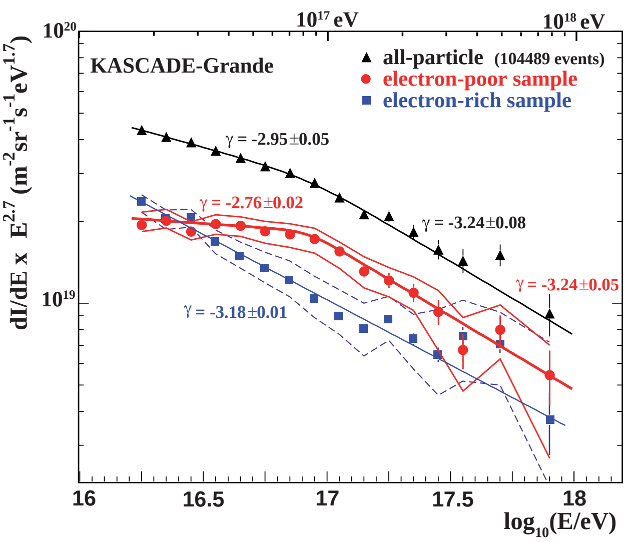

Figure 4: Reconstructed energy spectrum of the electron-poor and electron-rich components together with the all-particle spectrum for the angular range $0° - 40°$. The error bars show the statistical uncertainties; the bands assign systematic uncertainties due to selection of the subsamples.

area has been defined, essentially accepting events at larger distances from the muon detector (i.e. from the KASCADE array, see figure 1). The main effect of this event selection is that the 100% efficiency is reached at higher energies, that is not a problem for this analysis aimed to study a possible spectral feature at energies greater than $10^{17} eV$. In order to emphasize features of the light mass group we redefine the cut on the k parameter as $k_{er}(E) \leq (k_C(He) + k_C(E))/2$ (again a simulation based on the QGSJetII-02 hadronic interaction model is used). The obtained spectrum is shown in figure 5; a hardening, or ankle-like feature, is clearly observed. Fitting this spectrum with the same function used for the all-particle and heavy mass groups primary spectra we obtain a change of the spectral index from $\gamma = -3.25 \pm 0.05$ to $\gamma = -2.79 \pm 0.08$ at an energy of $\log_{10}(E/eV) = 17.08 \pm 0.08$. The measured number of events above the bending is $N_{meas} = 595$. Without the bending we would expect $N_{exp} = 467$ events above this ankle-like feature. The Poisson probability to measure at least N_{meas} events above the bending, if N_{exp} are expected is $P \sim 7.23 \times 10^{-9}$, corresponding to a 5.8σ significance.

Comparing the two previous observations it is important to notice that the knee in the heavy component occurs at a lower energy compared to the bending in the spectrum of the light primaries. Therefore the steepening of the heavy spectrum and the recovery of the light component are not due to a bias in the reconstruction or separation procedures. It is worth pointing out that the slope of the heavy mass spectrum above the knee-like feature is very similar to the slope of the light mass spectrum before the ankle-like feature. The slope index of the light mass group spectrum above the ankle-like feature is $\gamma \sim -2.7$ and this can be interpreted as an indication of an injection of a new (extragalactic) population of high energy cosmic-rays[5].

3.3. Energy spectra for elemental groups by unfolding analysis

The measured two-dimensional shower size spectrum of the number of charged particles ($\log_{10}(N_{ch})$) vs. the number of muons ($\log_{10}(N_\mu)$) is the basis for the unfolding analysis[1] to

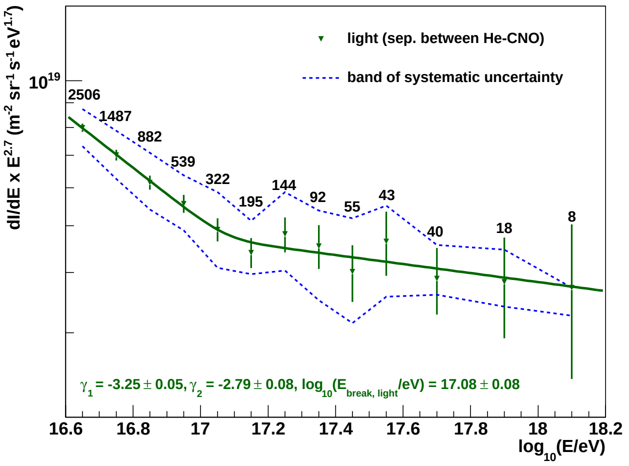

Figure 5: The reconstructed energy spectrum of the light mass component of cosmic rays. The number of events per energy bin is indicated as well as the range of systematic uncertainty. The error bars show the statistical uncertainties.

infer the absolute fluxes of different mass groups. With the KASCADE-Grande resolution we can separate five different groups. Only events with shower sizes for which the experiment is fully efficient are considered, i.e. $\log_{10}(N_{ch}) \geq 6.0$ and $\log_{10}(N_{\mu}) \geq 5.0$. In order to avoid effects due to the varying attenuation of the shower sizes for different angles of incidence, the data set used is restricted to showers with zenith angles $\theta \leq 18°$.

The analysis objective is to compute the energy spectra of five cosmic ray mass groups[7](represented by protons (p), helium (He), carbon (C), silicon (Si), and iron (Fe) nuclei) from $10^{16}eV$ to $10^{17}eV$ primary energies. The convolution of the sought-after differential fluxes $dJ_n/d\log_{10} E$ of the primary cosmic ray nuclei n into the measured number of showers N_i contributing to the cell i of shower size plane, and thus to the content of this specific charged particle and muon number bin $(\log_{10}(N_{ch}); \log_{10}(N_{\mu}))$ in the previously mentioned bi-dimensional spectra, can be described by an integral equation:

$$N_i = 2\pi A_f T_m \sum_{n=1}^{N_{nucl}} \int_{0°}^{18°} \int_{-\infty}^{+\infty} \frac{dJ_n}{d\log_{10} E}\, p_n\, sin\theta\, cos\theta\, d\log_{10} E\, d\theta \quad (4)$$

One has to sum over all N_{nucl} elements contributing to the all-particle cosmic ray spectrum, in this analysis the five representative primaries. T_m is the measurement time, the factor 2π accounts for the integration over the azimuth angle, and A_f is the chosen fiducial area. The term p_n represents the conditional probability to reconstruct a certain combination of charged particle and muon number respectively (i.e. to get an entry in the cell $(\log_{10}(N_{ch}); \log_{10}(N_{\mu}))$ if the air shower inducing particle was of the type n and had an energy E.

In figure 6, the unfolded differential energy spectra of lighter primaries (protons as well as helium and carbon nuclei, upper panel), and the spectra of heavier ones (silicon and iron nuclei, lower panel) are depicted. In addition, all five unfolded spectra are summed up to the all-particle flux, which is also shown. The shaded band indicates the methodical uncertainties, while the error bars represent the statistical error originating from the limited measurement time. The uncertainties due to the interaction models used, i.e. of QGSJET-II-02 and FLUKA2002.4[20], cannot be considered.

With increasing energy the heavy component gets the dominant contributor to the cosmic ray composition. The spectra of lighter primaries are rather featureless within the given uncertainties, while in the iron spectrum there is a slight bending discernible at around $10^{17}eV$. The position of this knee-like structure agrees with those observed in the all-particle and in the heavy component spectra previously discussed.

There are no indications so far that the interaction models used, i.e. QGSJET-II-02 and FLUKA 2002.4, have serious deficits in the description of the physics of hadronic interactions at these energies, which, however, does not mean necessarily that these models must be accurate in all details. Different interaction models primarily have impact on the absolute scale of energy and masses, such that model uncertainties can shift the unfolded spectra, possibly resulting in different abundances of the primaries, while specific structures, e.g. knee-like features of the spectra, are less affected by the models.

3.4. Large Scale Anisotropies

The search for large scale anisotropies has been performed through a differential method, the so called East-West[3] method, based on the counting rate differences between East-ward and West-ward directions. This method allows to remove counting rate variations caused by atmospheric and instrumental effects. The used data set contains 10^7 events recorded between December 2003 and October 2011. To ensure reconstruction quality, a cut on the zenith angle θ and on the number of charged particles at observation level (N_{ch}) was applied: $\theta < 40°$ and $Log(Nch) > 5.2$.

Figure 7 shows the modulation in sidereal[5] time obtained using the East-West method. The amplitude of the first harmonic calculated in sidereal time is $(0.28 \pm 0.08) \times 10^{-2}$ with a 0.2% Rayleigh probability of being due to background fluctuation (i.e. $\sigma = 3.5$) at median energy $3.3 \times 10^{15}eV$. The 99% C.L. upper limit on the amplitude is 0.47×10^{-2}, derived according to the distribution drawn from a population characterized by an anisotropy of unknown amplitude and phase as derived by Linsley[21].

To investigate a variation of the amplitude and phase of the first harmonic with primary energy we have performed the same analysis in intervals of the number of charged particles. In order to have bins containing events of similar energy and have good statistics in each of them we have chosen $\Delta LogN_{ch} = 0.4$. The results are shown in table 1, in none of the bins the amplitude of the harmonic is statistically significant and so we have calculated the upper limits at 99% confidence level. The N_{ch} limits

[5]sidereal time: Common time scale among astronomers which is based on the Earth's rotation measured relative to the fixed stars.

of the intervals used for the harmonic analysis are converted to primary energy and the median energy of the events in each bin is defined as representative energy.

$\log_{10}(N_{ch})$	E (PeV)	$A_{sid} \times 10^{-2}$	hours
5.2-5.6	2.6×10^{15}	0.26 ± 0.10	15 ± 1.4
5.6-6	5.5×10^{15}	0.39 ± 0.17	16.3 ± 1.6
6.0-6.4	1.2×10^{16}	0.67 ± 0.41	8.4 ± 2.2
6.4-6.8	2.5×10^{16}	0.5 ± 1.0	18.4 ± 6.6
> 6.8	6.3×10^{16}	4.6 ± 2.2	16.1 ± 1.8

$\log_{10}(N_{ch})$	E (PeV)	U.L. 10^{-2}	P %
5.2-5.6	2.6×10^{15}	0.49	3
5.6-6	5.5×10^{15}	0.77	7
6.0-6.4	1.2×10^{16}	1.54	26
6.4-6.8	2.5×10^{16}	2.8	85
> 6.8	6.3×10^{16}	9.3	11

Table 1: Results of harmonic analysis through the East-West method for five intervals of N_{ch}.

4. Conclusions

The KASCADE-Grande experiment took data from January 2004 to end 2012, detecting EAS generated by primary cosmic rays in the $10^{16} - 10^{18} eV$ energy range. In this contribution we have shown the main results obtained so far by the experiment:

1. a measurement of the all-particle energy spectrum, showing that it cannot be described by a single slope power law. A hardening slightly above $10^{16} eV$ and a steepening at $\log_{10}(E/eV) = 16.92 \pm 0.10$ are detected.
2. The measurement of the light and heavy primary mass group energy spectra. These spectra were obtained dividing the events in two samples on the basis of the ratio between the muon and the charged particles numbers. A steepening at $\log_{10}(E/eV) = 16.92 \pm 0.04$ in the spectrum of the electron poor event sample (heavy primaries) and a hardening at $\log_{10}(E/eV) = 17.08 \pm 0.08$ in the one of the electron rich (light primaries) one were observed. The slope of the heavy mass group spectrum above the knee-like feature is similar to the one of the light mass spectrum before the the ankle-like feature.
3. Applying the unfolding algorithm to the $N_{ch} vs N_{\mu}$ spectrum we could extract the spectra of five different elemental mass groups. These measurement relies on the hadronic interaction model utilized in the EAS simulation. Making use of the same hadronic interaction model to interpret the data, the measured fluxes are in agreement with those obtained at lower energies by the KASCADE array and with the findings above for the KASCADE-Grande energy range.
4. Upper limits on the amplitude of large scale anisotropies in four N_{ch} bins.

Acknowledgment: The authors would like to thank the members of the engineering and technical staff of the KASCADE-Grande collaboration, who contributed to the success of the experiment. The KASCADE-Grande experiment is supported in Germany by the BMBF and by the Helmholtz Alliance for Astroparticle Physics - HAP funded by the Initiative and Networking Fund of the Helmholtz Association, by the MIUR and INAF of Italy, the Polish Ministry of Science and Higher Education, and the Romanian Authority for Scientific Research UEFISCDI (PNII-IDEI grants 271/2011 and 17/2011).

References

[1] T. Antoni et al., Astropart. Phys. **24**, 1 (2005).
[2] M. Aglietta et al., Astropart. Phys. **10**, 1 (1999).
[3] R. Bonino et al., Astrophys. J. **738** (2011) 67-84.
[4] W.D. Apel et al., Astropart. Phys. **36**, 183 (2012)
[5] W.-D. Apel et al., Phys. Rev. D **87**, 081101 (2013).
[6] W.D. Apel et al., Phys. Rev. Lett. **107**, 171104 (2011).
[7] W.D. Apel et al., Astropart. Phys. **47**, 54-66 (2013).
[8] C. Curcio et al. (KASCADE-Grande collaboration), Proc. of the 33rd ICRC (Rio de Janeiro), (2013).
[9] T. Antoni et al., Nucl. Instr. & Meth. A **513**, 490 (2003).
[10] W.D. Apel et al., Nucl. Instr. & Meth. A **620**, 202 (2010).
[11] W.D. Apel et al, KASCADE-Grande contributions to the 32nd ICRC, Beijing, China astro-ph/1111.5436v1 (2011).
[12] S. Ostapchenko, Nucl. Phys. B (Proc. Suppl.) **151** (2006) 143.
[13] L. Kuzmichev et al., Proc. 32nd Int. Cosmic Ray Conf. (Beijing) **1**, 209 (2011).
[14] M.G. Aartsen et al., arXiv:1307.3795.
[15] W.D. Apel et al., J. Adv. Space Res., http//dx.doi.org/10.1016/j.asr.2013.05.008 (2013).
[16] E.-J. Ahn et al., Phys. Rev. D **80**, 094003 (2009).
[17] K. Werner. Nucl. Phys. B (Proc. Suppl.) **175** (2008) 81.
[18] S. Ostapchenko, Phys Rev D **83** (2011) 014018.
[19] T. Antoni et al., Astropart. Phys. **16**, 245 (2002).
[20] G. Battistoni et al., AIP Conf. Proc. **896** (2007) 31-49.
[21] J. Linsley, Phys. Rev. Lett. **34** (1975) 1530.

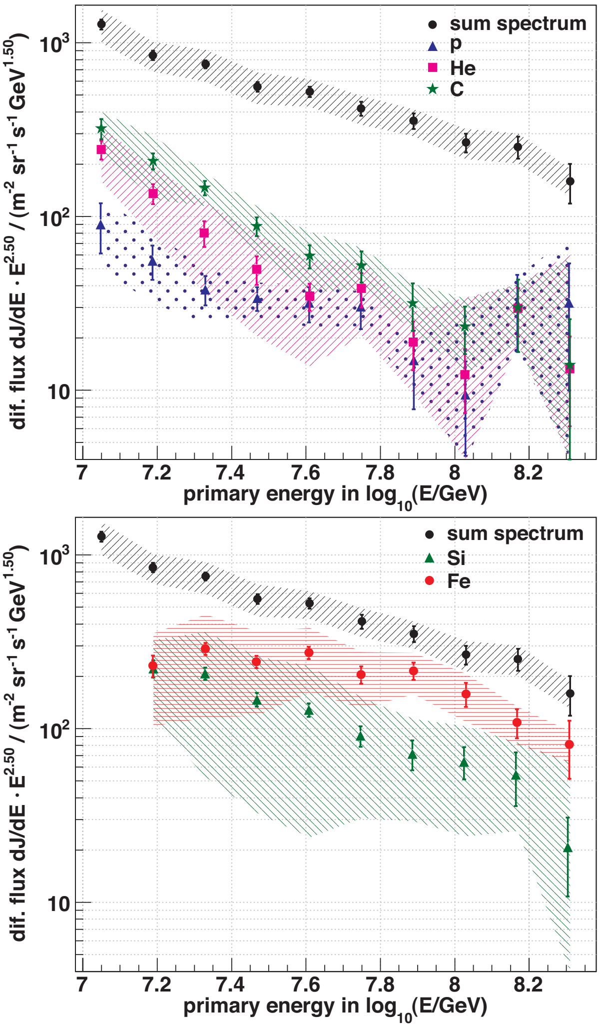

Figure 6: The unfolded energy spectra for elemental groups of cosmic rays, represented by protons, helium, and carbon nuclei (upper panel) as well as by silicon and iron nuclei (lower panel), based on KASCADE-Grande measurements. The all-particle spectrum that is the sum of all five individual spectra is also shown. The error bars represent the statistical uncertainties, while the error bands mark the maximal range of systematic uncertainties. The response matrix used is based on the interaction models QGSJetII-02[12] and FLUKA 2002.4[20]

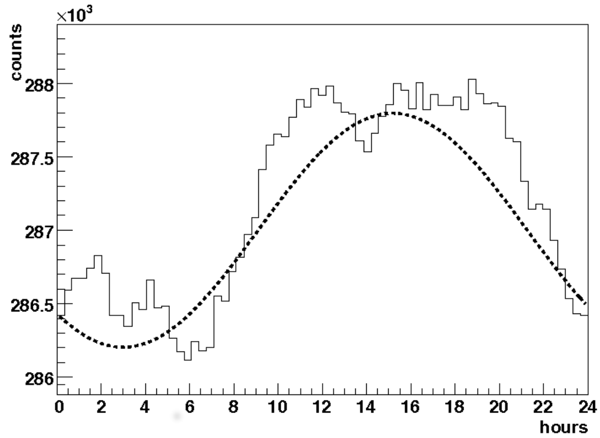

Figure 7: Sidereal time distribution of the number of counts ($\theta < 40°$ and $LogN_{ch} > 5.2$) in 20 minutes intervals obtained applying the East-West method. The dashed line shows the calculated first harmonic.